

# Upregulation of the $\text{Na}^+$ -Coupled Phosphate Cotransporters NaPi-IIa and NaPi-IIb by B-RAF

Tatsiana Pakladok · Zohreh Hosseinzadeh · Aleksandra Lebedeva · Ioana Alesutan · Florian Lang

Received: 20 August 2013 / Accepted: 8 November 2013 / Published online: 21 November 2013  
© Springer Science+Business Media New York 2013

**Abstract** B-RAF, a serine/threonine protein kinase, contributes to signaling of insulin-like growth factor IGF1. Effects of IGF1 include stimulation of proximal renal tubular phosphate transport, accomplished in large part by  $\text{Na}^+$ -coupled phosphate cotransporter NaPi-IIa. The related  $\text{Na}^+$ -coupled phosphate cotransporter NaPi-IIb accomplishes phosphate transport in intestine and tumor cells. The present study explored whether B-RAF influences protein abundance and/or activity of type II  $\text{Na}^+$ -coupled phosphate cotransporters NaPi-IIa and NaPi-IIb. cRNA encoding wild-type NaPi-IIa and wild-type NaPi-IIb was injected into *Xenopus* oocytes with or without additional injection of cRNA encoding wild-type B-RAF, and electrogenic phosphate transport determined by dual-electrode voltage clamp. NaPi-IIa protein abundance in *Xenopus* oocyte cell membrane was visualized by confocal microscopy and quantified by chemiluminescence. Moreover, in HEK293 cells, the effect of B-RAF inhibitor PLX-4720 on NaPi-IIa cell surface protein abundance was quantified utilizing biotinylation of cell surface proteins and western blotting. In NaPi-IIa-expressing *Xenopus* oocytes, but not in oocytes injected with water, addition of phosphate to extracellular bath generated a current ( $I_p$ ), which was significantly increased following coexpression of B-RAF. According to kinetic analysis, coexpression of B-RAF enhanced the maximal  $I_p$ . Coexpression of B-RAF further enhanced NaPi-IIa protein

abundance in the *Xenopus* oocyte cell membrane. Treatment of HEK293 cells for 24 h with PLX-4720 significantly decreased NaPi-IIa cell membrane protein abundance. Coexpression of B-RAF, further significantly increased  $I_p$  in NaPi-IIb-expressing *Xenopus* oocytes. Again, B-RAF coexpression enhanced the maximal  $I_p$ . In conclusion, B-RAF is a powerful stimulator of the renal and intestinal type II  $\text{Na}^+$ -coupled phosphate cotransporters NaPi-IIa and NaPi-IIb, respectively.

**Keywords** Phosphate uptake · Renal tubule · Intestine · B-RAF · NaPi-IIa · NaPi-IIb · HEK293 cells

## Introduction

Phosphate transport across the apical brush border membrane of proximal renal tubules is accomplished in large part by the type II  $\text{Na}^+$ -coupled phosphate cotransporter NaPi-IIa (SLC34A1) (Biber et al. 2009; Murer et al. 2004; Villa-Bellosta et al. 2009). Renal tubular phosphate reabsorption is under tight regulation by phosphate balance, acid–base status, and several hormones, including parathyroid hormone, 1,25-(OH)<sub>2</sub> vitamin D<sub>3</sub>, FGF23, insulin, and insulin-like growth factor IGF1 (Allon 1992; DeFronzo et al. 1976; Feld and Hirschberg 1996; Jehle et al. 1998; Murer et al. 2000; Nowik et al. 2008; Parkin and Bray 2006). NaPi-IIa-regulating signaling molecules include: klotho, protein kinases A and C, PI3K/PKB/GSK-3 kinase cascade, and ERK1/2 (Bacic et al. 2006, 2003; Bhandaru et al. 2011; Dermaku-Sopjani et al. 2011; Foller et al. 2011; Hu et al. 2010; Kempe et al. 2010a, b).

In intestine, transport of inorganic phosphate is accomplished in large part by the type II  $\text{Na}^+$ -coupled phosphate

T. Pakladok · Z. Hosseinzadeh · A. Lebedeva · I. Alesutan · F. Lang (✉)  
Department of Physiology I, University of Tübingen,  
Gmelinstr. 5, 72076 Tübingen, Germany  
e-mail: florian.lang@uni-tuebingen.de

A. Lebedeva  
Department of Immunology, Institute of Experimental Medicine,  
St. Petersburg, Russia

cotransporter NaPi-IIb (SLC34A2) (Marks et al. 2010). NaPi-IIb expression is highest in the small intestine (Marks et al. 2010). Mutations in the SLC34A2 gene are leading to accumulation of phosphate in lung which causes pulmonary alveolar microlithiasis (Ferreira Francisco et al. 2013). Expression of SLC34A2 was further detected in ovarian, papillary thyroid, and breast cancer (Chen et al. 2010; Jarzab et al. 2005; Rangel et al. 2003). Similar to NaPi-IIa, NaPi-IIb is regulated by growth factors (Xu et al. 2003), and phosphate transport was shown to play an important role in cell proliferation (Beck et al. 2009; Nielsen et al. 2001).

Growth factor signaling involves B-RAF (Murillo-Cuesta et al. 2011), a serine/threonine kinase, upregulated in a variety of tumor cells (Davies et al. 2002; De Luca et al. 2012; Kamata and Pritchard 2011; Roring and Brummer 2012). The kinase plays a critical role in the activation of the RAS/RAF/MEK/ERK pathway, which participates in the regulation of cell proliferation, differentiation, and survival (Eisenhardt et al. 2011). B-RAF is activated by point mutations in human cancer, in 90 % of the cases having a valine replaced by glutamate in the activation segment, now referred to as V600E (Davies et al. 2002; Wan et al. 2004). Growth of cancer cells with the V600E mutation does not require activation of RAS (Davies et al. 2002). In kidney, B-RAF participates in the pathophysiology of polycystic kidney disease (PKD) (Wallace 2011). PKD cells lack the  $\text{Ca}^{2+}$  and AKT-dependent inhibition of B-RAF leading to enhanced activity of B-RAF and subsequent stimulation of cell proliferation (Wallace 2011). Considering the role of B-RAF in tumors and in the pathophysiology of polycystic kidney disease, we hypothesized that B-RAF may participate in the regulation of the type II sodium-dependent phosphate cotransporters.

The present study thus explored the putative role of B-RAF in the regulation of NaPi-IIa or NaPi-IIb. To this end, NaPi-IIa or NaPi-IIb was expressed in *Xenopus* oocytes with or without additional coexpression of B-RAF and the phosphate-induced current, reflecting electrogenic phosphate transport across the cell membrane, determined utilizing dual-electrode voltage clamp. As a result, coexpression of B-RAF indeed enhanced phosphate-induced currents in NaPi-IIa- or NaPi-IIb expressing *Xenopus* oocytes. Immunocytochemistry with confocal microscopy and chemiluminescence revealed that B-RAF increased the NaPi-IIa protein abundance in the cell membrane. Moreover, biotinylation of cell surface proteins has been employed to quantify the effect of B-RAF inhibitor PLX-4720 on NaPi-IIa cell membrane expression in HEK293 cells which have previously been shown to express NaPi-IIa transporters (Tanner et al. 2007). As a result, B-RAF proved to upregulate the protein abundance of the type IIa  $\text{Na}^+$ -coupled phosphate cotransporter.

## Materials and Methods

### Constructs

For generation of cRNA, constructs were used encoding wild-type human NaPi-IIa (Busch et al. 1995), wild-type mouse NaPi-IIb (Dermaku-Sopjani et al. 2011; Hilfiker et al. 1998), and wild-type human B-RAF (Pakladok et al. 2012). The constructs were used for generation of cRNA, as described previously (Broer et al. 1994; Hosseinzadeh et al. 2013b).

### Voltage Clamp in *Xenopus* Oocytes

*Xenopus* oocytes were prepared, as previously described (Munoz et al. 2013; Shojaiefard et al. 2012). The oocytes were injected with 10 ng cRNA encoding wild-type NaPi-IIa or 15 ng cRNA encoding wild-type NaPi-IIb and 10 ng cRNA encoding wild-type B-RAF on the same day (Almilaji et al. 2013a; Hosseinzadeh et al. 2013a). For control, the oocytes were injected with the respective volumes of water. The oocytes were maintained at 17 °C in ND96 solution containing in mM: 96 NaCl, 2 KCl, 1.0  $\text{MgCl}_2$ , 1.8  $\text{CaCl}_2$ , 5 HEPES, 0.11 tetracycline (Sigma, Steinheim, Germany), 4  $\mu\text{M}$  ciprofloxacin (Fresenius, Bad Homburg, Germany), 0.2 refobacin (MerckSerono, Darmstadt, Germany), and 0.5 theophylline (Takeda, Singen, Germany) as well as 5 mM sodium pyruvate (Sigma, Steinheim, Germany) (Almilaji et al. 2013b; Bogatikov et al. 2012). The pH was adjusted to 7.4 by addition of NaOH. The voltage clamp experiments were performed at room temperature, 3–4 days after injection. Two-electrode voltage clamp recordings (Strutz-Seebohm et al. 2011) were performed at a holding potential of  $-60$  mV. The data were filtered at 10 Hz, and recorded with a Digidata A/D-D/A converter and Clampex 9.2 software for data acquisition and analysis (Axon Instruments). The control superfusate (ND96) contained 96 mM NaCl, 2 mM KCl, 1.8 mM  $\text{CaCl}_2$ , 1 mM  $\text{MgCl}_2$ , and 5 mM HEPES, pH 7.4 (Alesutan et al. 2012; Hosseinzadeh et al. 2012a). Phosphate was added to the solutions at a concentration of 1 mM, unless otherwise stated. The flow rate of the superfusion was approx. 20 ml/min, and a complete exchange of the bath solution was reached within about 10 s (Henrion et al. 2012; Hosseinzadeh et al. 2012b).

### Detection of NaPi-IIa Cell Surface Expression by Chemiluminescence

To determine NaPi-IIa cell surface expression by chemiluminescence (Alesutan et al. 2011), the oocytes were incubated with primary rabbit anti-human SLC34A1 (NaPi-IIa) polyclonal antibody (1:500, Life Span Biosciences, WA,

USA) and subsequently with secondary HRP-conjugated goat anti-rabbit IgG antibody (1:1000, Cell Signaling Technology, MA, USA). Individual oocytes were placed in 96 well plates with 20  $\mu$ l of SuperSignal ELISA Femto Maximum Sensitivity Substrate (Pierce, Rockford, IL, USA), and chemiluminescence of single oocytes was quantified in a luminometer (Walter Wallac 2 plate reader, Perkin Elmer, Juegesheim, Germany) by integrating the signal over a period of 1 s (Warsi et al. 2013). Results display normalized relative light units (Alesutan et al. 2010). Integrity of the measured oocytes was assessed by visual control after the measurement to avoid unspecific light signals from the cytosol.

#### Immunocytochemistry and Confocal Microscopy

After 4 % paraformaldehyde fixation for at least 4 h, oocytes were cryoprotected in 30 % sucrose, frozen in mounting medium and placed on a cryostat (Pakladok et al. 2013). Sections were collected at a thickness of 8  $\mu$ m on coated slides and stored at  $-20^{\circ}\text{C}$ . For immunostaining, sections were dried at room temperature, fixed in acetone/methanol (1:1) for 15 min, washed in PBS, and blocked for 1 h in 1 % bovine serum albumin in PBS. The primary antibody used was rabbit anti-human SLC34A1 (NaPi-IIa) polyclonal antibody (1:100, Life Span Biosciences, WA, USA). Incubation was performed in a moist chamber overnight at  $4^{\circ}\text{C}$ . The binding of primary antibody was visualized with FITC-conjugated goat anti-rabbit IgG (1:1000, Invitrogen, Molecular Probes, Eugene, OR, USA). Next, oocytes were analyzed by the fluorescence laser scanning microscope (LSM 510; CarlZeiss MicroImaging, Göttingen, Germany) with A-Plan 40x/1.2 W DICIII (Mia et al. 2012). Brightness and contrast settings were kept constant during imaging of all oocytes in each injection series.

#### Cell Culture of HEK293 Cells

Human embryonic kidney cells (HEK293) were cultured in Dulbecco's Modified Eagle Medium DMEM, containing 4.5 g/l glucose (Gibco, Life Technologies GmbH, Germany), supplemented with 2 mM L-glutamine (PAA Laboratories GmbH, Germany), 10 % FBS (PAA Laboratories GmbH, Germany), 100 U/ml penicillin, and 100  $\mu$ g/ml streptomycin (PAA Laboratories GmbH, Germany). Where indicated, cells were treated 24 h with 10  $\mu$ M B-RAF inhibitor PLX-4720 (Selleck Chemicals, USA) dissolved in DMSO. Equal amounts of DMSO were used as control.

#### Biotinylation of Cell Surface Proteins

To analyze NaPi-IIa cell membrane abundance, HEK293 cells were washed twice with ice-cold PBS and labeled with

250  $\mu$ g/ml Sulfo-NHS-LC-biotin (Pierce, Rockford, IL, USA) in PBS for 30 min at  $4^{\circ}\text{C}$ . The Sulfo-NHS-LC-biotin bound to the membrane proteins was quenched with 50 mM Tris-HCl buffer pH 7.4. After washing, HEK293 cells were lysed with ice-cold RIPA buffer (Cell Signaling, Danvers, MA, USA), supplemented with complete protease and phosphatase inhibitor cocktail (Thermo Fisher Scientific, Rockford, IL, USA). After centrifugation at 10,000 rpm for 5 min, 300  $\mu$ g of proteins were supplemented with 50  $\mu$ l washed immobilized Neutravidin Agarose beads (Pierce, Rockford, IL, USA) and incubated at  $4^{\circ}\text{C}$  overnight on a rotator. The beads were then pelleted by a 1 min centrifugation at 13,000 rpm and washed 3 times in PBS containing 1 % NP-40/0.1 % SDS and twice in 0.1 % NP-40/0.5 M NaCl. Proteins were solubilized in Roti-Load1 buffer (Carl Roth GmbH, Karlsruhe, Germany) at  $95^{\circ}\text{C}$  for 10 min, separated on 10 % SDS-polyacrylamide gels and transferred to PVDF membranes. After blocking with 5 % nonfat dry milk in TBS 0.1 % Tween20 for 1 h at room temperature, the blots were incubated overnight at  $4^{\circ}\text{C}$  with rabbit anti-human SLC34A1 (NaPi-IIa) polyclonal antibody (diluted 1:500, Life Span Biosciences, WA, USA). After washing (TBST), blots were incubated with anti-rabbit HRP-conjugated antibody (diluted 1:1000, Cell Signaling, Danvers, MA, USA) for 1 h at RT. Antibody binding was detected with the ECL detection reagent (Amersham, Freiburg, Germany). Bands were quantified with Quantity One Software (Bio-Rad, Muenchen, Germany) and results are shown normalized to the control treated group.

#### Statistical Analysis

Data are provided as mean  $\pm$  SEM,  $n$  represents the number of oocytes investigated. All experiments were repeated with at least three batches of oocytes; in all repetitions qualitatively similar data were obtained. All data were tested for significance using Kruskal-Wallis test or unpaired Student's  $t$  test, where appropriate. Only results with  $p < 0.05$  were considered statistically significant.

#### Results

In the first series of experiments, we explored whether B-RAF influences the activity of the renal type II  $\text{Na}^+$ -coupled phosphate cotransporter NaPi-IIa. To this end, the cotransporter was expressed in *Xenopus* oocytes with or without additional coexpression of wild-type B-RAF. Phosphate transport was estimated from the current generated, following addition of phosphate to extracellular fluid. The substrate-induced current was determined utilizing dual-electrode voltage clamp. As illustrated in Fig. 1, addition of phosphate (1 mM) to the bath solution did not

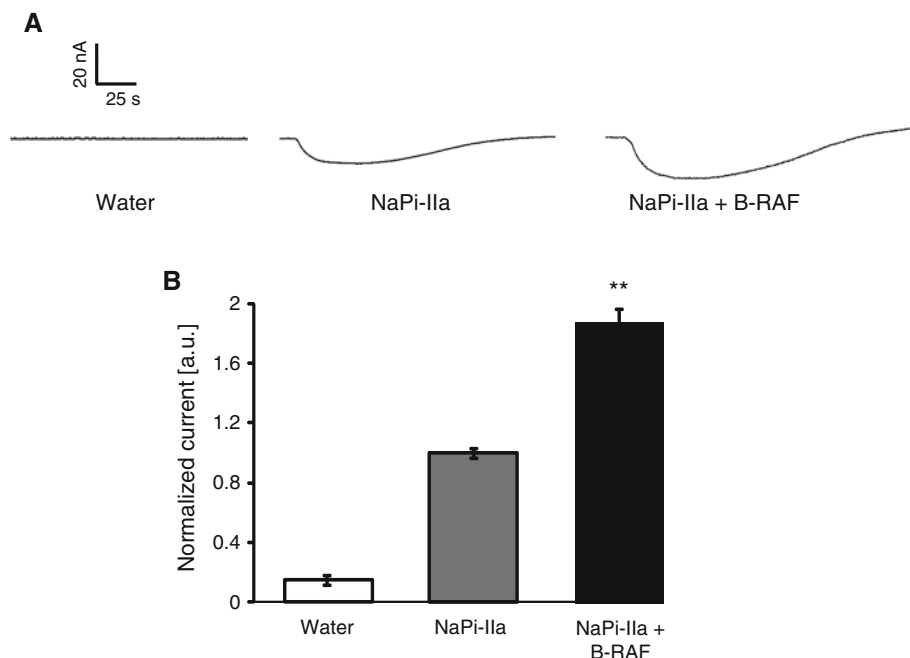


**Fig. 1** Coexpression of B-RAF increased electrogenic phosphate transport in NaPi-IIa-expressing *Xenopus* oocytes. **a** Representative original tracings showing phosphate-induced current (1 mM) ( $I_P$ ) in *Xenopus* oocytes injected with water (Water), expressing NaPi-IIa without (NaPi-IIa) or with additional coexpression of wild-type B-RAF (NaPi-IIa + B-

RAF). **b** Arithmetic mean  $\pm$  SEM ( $n = 14\text{--}17$ ) of normalized phosphate-induced current ( $I_P$ ) in *Xenopus* oocytes injected with water (white bar), expressing NaPi-IIa without (gray bar) or with additional coexpression of wild-type B-RAF (black bar). \*\* $p < 0.01$  indicates statistically significant difference from *Xenopus* oocytes expressing NaPi-IIa alone

induce an appreciable inward current in water-injected *Xenopus* oocytes. Thus, *Xenopus* oocytes do not express appreciable endogenous electrogenic phosphate transporters. In *Xenopus* oocytes expressing NaPi-IIa, however, phosphate induced an inward current ( $I_P$ ) reflecting electrogenic entry of  $\text{Na}^+$  and phosphate. As shown in Fig. 1,  $I_P$  was significantly enhanced by additional coexpression of wild-type B-RAF in NaPi-IIa-expressing *Xenopus* oocytes.

In theory, B-RAF could have been effective by increasing maximal transport rate or by enhancing the affinity of the carrier. To discriminate between those two possibilities, kinetic analysis of the phosphate-induced currents was performed. As illustrated in Fig. 2, phosphate transport was saturable at increasing substrate concentrations. Kinetic analysis yielded a maximal  $I_P$  of  $16.25 \pm 0.12$  nA ( $n = 12$ ) in *Xenopus* oocytes expressing NaPi-IIa alone. Coexpression of wild-type B-RAF, significantly enhanced the maximal  $I_P$  to  $29.09 \pm 0.30$  nA ( $n = 12$ ). Calculation of the phosphate concentration required for halfmaximal  $I_P$  ( $K_M$ ) yielded values of  $1046.61 \pm 43.96$   $\mu\text{M}$  ( $n = 12$ ) in *Xenopus* oocytes expressing NaPi-IIa alone and of  $785.60 \pm 21.94$   $\mu\text{M}$  ( $n = 12$ ) in *Xenopus* oocytes expressing NaPi-IIa together with B-RAF, values again significantly different. As a result, coexpression of wild-type B-RAF enhanced NaPi-IIa activity by increasing the maximal current and by enhancing the affinity of the carrier.

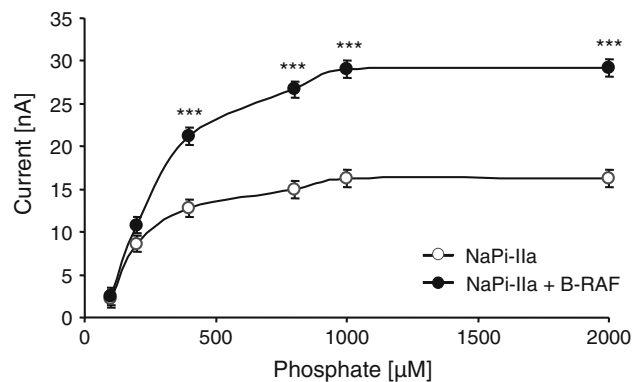


**Fig. 2** Coexpression of B-RAF increased maximal phosphate transport rate in NaPi-IIa-expressing *Xenopus* oocytes. Arithmetic mean  $\pm$  SEM ( $n = 12$ ) of phosphate-induced current ( $I_P$ , nA) as a function of phosphate concentration in *Xenopus* oocytes expressing NaPi-IIa without (open circles) and with additional coexpression of wild-type B-RAF (closed circles). \*\*\* $p < 0.001$  indicates statistically significant difference from *Xenopus* oocytes expressing NaPi-IIa alone at the respective phosphate concentrations

Enhanced maximal NaPi-IIa activity could have resulted from increased carrier protein abundance in the plasma membrane. Immunocytochemistry with confocal microscopy was thus employed to visualize the NaPi-IIa protein abundance in the cell membrane. As shown in Fig. 3a, the coexpression of wild-type B-RAF was followed by an

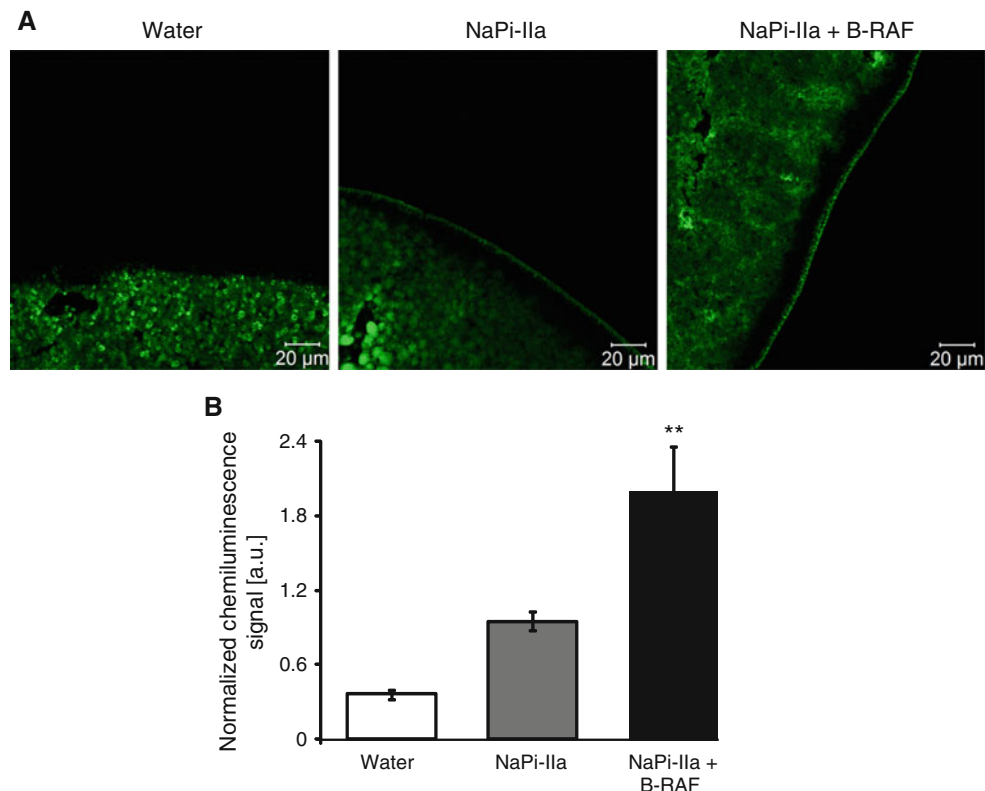


**Fig. 3** Coexpression of B-RAF enhanced NaPi-IIa protein abundance at the cell surface in NaPi-IIa-expressing *Xenopus* oocytes. **a** Confocal images reflecting NaPi-IIa membrane protein abundance in *Xenopus* oocytes injected with water (Water), expressing NaPi-IIa without (NaPi-IIa) or with additional coexpression of wild-type B-RAF (NaPi-IIa+B-RAF). The images are representative for three

independent experiments. **b** Arithmetic mean  $\pm$  SEM ( $n = 44$ –63) of the chemiluminescence of NaPi-IIa cell surface protein abundance in *Xenopus* oocytes injected with water (white bar), expressing NaPi-IIa without (gray bar) or with additional coexpression of wild-type B-RAF (black bar). \*\* $p < 0.01$  indicates statistically significant difference from *Xenopus* oocytes expressing NaPi-IIa alone

increase of NaPi-IIa protein abundance within the oocyte cell membrane. The protein abundance was quantified utilizing chemiluminescence. As shown in Fig. 3b, the coexpression of wild-type B-RAF was followed by a significant increase of chemiluminescence, again pointing to enhanced cell membrane NaPi-IIa protein abundance following coexpression of B-RAF in NaPi-IIa-expressing *Xenopus* oocytes.

In another series of experiments, we explored whether B-RAF similarly regulates the protein abundance of NaPi-IIa in HEK293 cells. To this end, HEK293 cells were treated for 24 h with 10  $\mu$ M of the B-RAF inhibitor PLX-4720, and NaPi-IIa cell membrane protein abundance was analysed by biotinylation of the cell surface proteins with subsequent western blotting. As illustrated in Fig. 4a, b, treatment of HEK293 cells with B-RAF inhibitor PLX-4720 was followed by a statistically significant decrease in NaPi-IIa cell membrane protein abundance as compared with HEK293 cells treated with vehicle alone. Thus, PLX-4720 treatment decreased NaPi-IIa cell membrane protein abundance in HEK293 cells.

Further experiments explored whether B-RAF similarly influences the activity of the related type II  $\text{Na}^+$ -coupled phosphate cotransporter NaPi-IIb. As illustrated in Fig. 5, addition of phosphate (1 mM) to the bath solution again did not induce an appreciable inward current in water-injected *Xenopus* oocytes. In *Xenopus* oocytes expressing NaPi-IIb, however, phosphate induced an inward current ( $I_P$ ), which was significantly increased by additional coexpression of wild-type B-RAF.

As illustrated in Fig. 6, phosphate transport was saturable at increasing substrate concentrations. Kinetic analysis yielded a maximal  $I_P$  of  $15.45 \pm 0.80$  nA ( $n = 10$ ) in *Xenopus* oocytes expressing NaPi-IIb alone. Coexpression of wild-type B-RAF again significantly enhanced the maximal  $I_P$  to  $24.48 \pm 0.93$  nA ( $n = 8$ –10). Calculation of the phosphate concentration required for halfmaximal  $I_P$  ( $K_M$ ) yielded values of  $828.96 \pm 22.83$   $\mu$ M ( $n = 10$ ) in *Xenopus* oocytes expressing NaPi-IIb alone and of  $645.40 \pm 14.03$   $\mu$ M ( $n = 8$ –10) in *Xenopus* oocytes expressing NaPi-IIb together with B-RAF, values again significantly different. As a result, coexpression of wild-

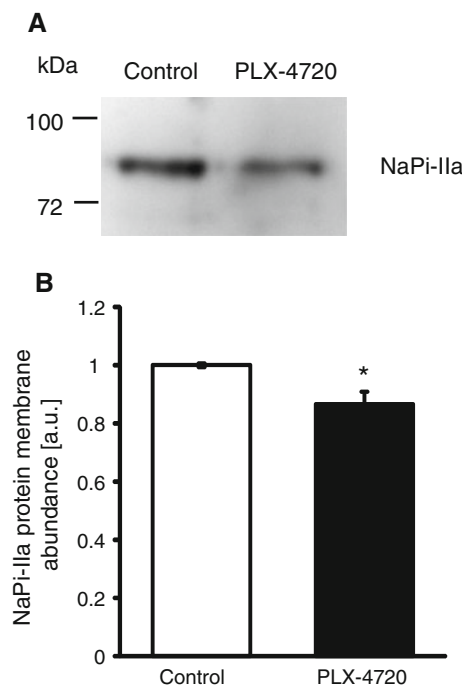


**Fig. 4** B-RAF inhibitor PLX-4720 decreased NaPi-IIa protein abundance at the cell surface in HEK293 cells. **a** Representative original western blot showing NaPi-IIa membrane protein abundance analysed by cell surface biotinylation in HEK293 cells after 24 h treatment with vehicle alone (Control) or with 10  $\mu$ M B-RAF inhibitor PLX-4720 (PLX-4720). **b** Arithmetic mean  $\pm$  SEM ( $n = 6$ ) of normalized NaPi-IIa membrane protein abundance analysed by cell surface biotinylation in HEK293 cells after 24 h treatment with vehicle alone (white bar) or with 10  $\mu$ M B-RAF inhibitor PLX-4720 (black bar). \* $p < 0.05$  indicates statistically significant difference from HEK293 cells treated with vehicle alone

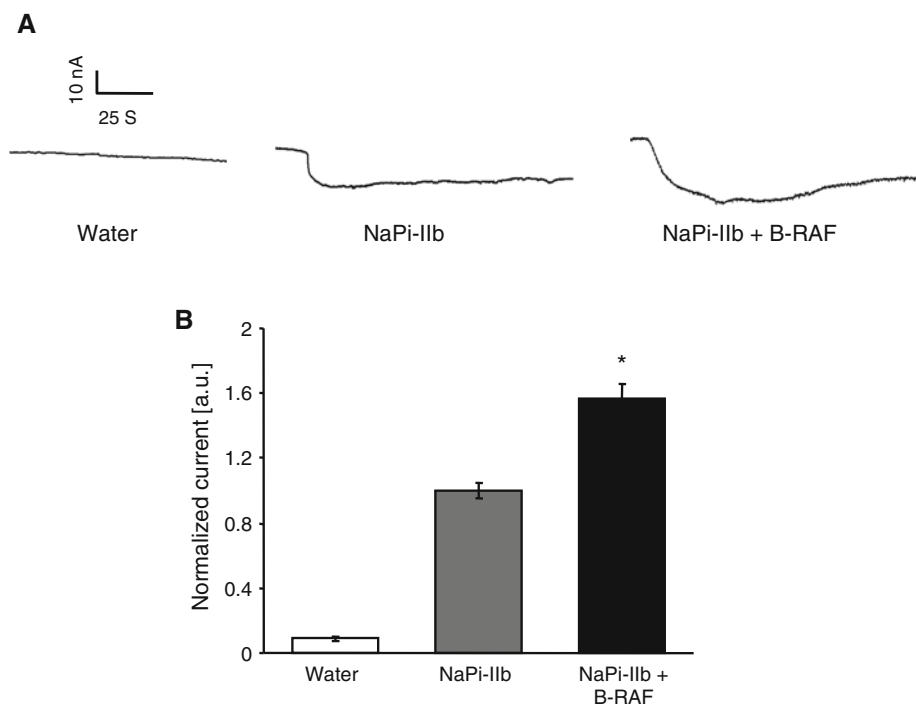
**Fig. 5** Coexpression of B-RAF increased electrogenic phosphate transport in NaPi-IIb-expressing *Xenopus* oocytes. **a** Representative original tracings showing phosphate-induced current (1 mM) ( $I_P$ ) in *Xenopus* oocytes injected with water (Water), expressing NaPi-IIb without (NaPi-IIb) or with additional coexpression of wild-type B-RAF (NaPi-IIb + B-RAF). **b** Arithmetic mean  $\pm$  SEM ( $n = 14$ ) of normalized phosphate-induced current ( $I_P$ ) in *Xenopus* oocytes injected with water (white bar), expressing NaPi-IIb without (gray bar) or with additional coexpression of wild-type B-RAF (black bar). \* $p < 0.05$  indicates statistically significant difference from *Xenopus* oocytes expressing NaPi-IIb alone

type B-RAF enhanced NaPi-IIb activity by increasing the maximal current and by enhancing the affinity of the carrier.

## Discussion

The present study reveals a novel signaling molecule in the regulation of  $\text{Na}^+$ -coupled phosphate cotransporters. Coexpression of the wild-type serine/threonine kinase B-RAF enhances NaPi-IIa phosphate-induced inward current ( $I_P$ ) in *Xenopus* oocytes. Furthermore, B-RAF enhances the NaPi-IIa protein abundance in the cell membrane, thus increasing the maximal electrogenic phosphate transport rate in NaPi-IIa-expressing *Xenopus* oocytes. Also, B-RAF significantly modified the substrate affinity of the carrier. Downregulation of NaPi-IIa protein abundance at the cell surface was observed in HEK293 cells following treatment with the B-RAF inhibitor PLX-4720, an observation again pointing to a role of B-RAF in the regulation of the  $\text{Na}^+$ -coupled phosphate cotransporter NaPi-IIa. It must be kept in mind, however, that the selectivity of the inhibitor may be limited. Coexpression of B-RAF similarly enhances NaPi-IIb phosphate-induced inward current ( $I_P$ ) by increasing the maximal electrogenic phosphate transport rate and by modifying the substrate affinity of the carrier in NaPi-IIb-expressing *Xenopus* oocytes. Thus, B-RAF regulates both members of the type II  $\text{Na}^+$ -coupled phosphate cotransporter family.

The present observations did not define the molecular mechanism involved in the regulation of carrier affinity and



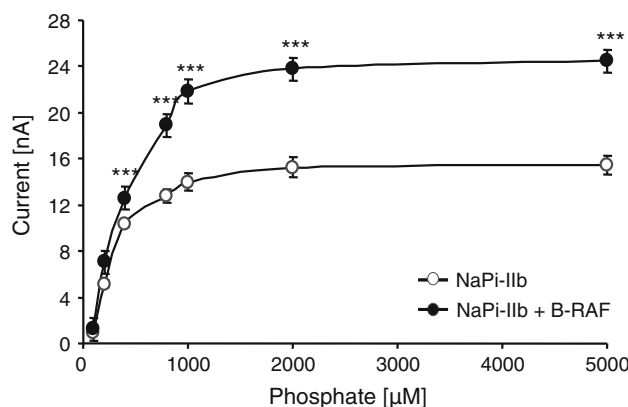


**Fig. 6** Coexpression of B-RAF increased maximal phosphate transport rate in NaPi-IIb-expressing *Xenopus* oocytes. Arithmetic mean  $\pm$  SEM ( $n = 10$ ) of phosphate-induced current ( $I_p$ , nA) as a function of phosphate concentration in *Xenopus* oocytes expressing NaPi-IIb without (open circles) and with additional coexpression of wild-type B-RAF (closed circles). \*\*\* $p < 0.001$  indicates statistically significant difference from *Xenopus* oocytes expressing NaPi-IIb alone at the respective phosphate concentrations

protein abundance in the cell membrane by B-RAF. In theory, B-RAF could exert its effects by directly phosphorylating the carrier or by phosphorylating other signaling molecules, which in turn modify carrier insertion and activity.

The present paper did not define the *in vivo* significance of B-RAF-sensitive regulation of the renal and intestinal type II  $\text{Na}^+$ -coupled phosphate cotransporters. B-RAF may be inhibited by AKT (protein kinase B) (Wallace 2011), a kinase similarly activated by IGF1 and stimulating the transport of glucose (Dieter et al. 2004; Ishiki and Klip 2005; Whiteman et al. 2002), amino acids (Carranza et al. 2008; Green et al. 2008; Lim et al. 2008),  $\text{Ca}^{2+}$  and  $\text{H}^+$  (Vaughan-Jones and Swietach 2008),  $\text{Na}^+$  (Lee et al. 2007),  $\text{K}^+$  (Mannack et al. 2008) as well as phosphate (Foller et al. 2011; Kempe et al. 2010a). Mice lacking Akt2 suffer from phosphaturia (Kempe et al. 2010a), an effect at least partially due to disinhibition of glycogen synthase kinase GSK-3 (Foller et al. 2011). Clearly, additional experimentation will be required to define the putative role of B-RAF signaling in the regulation of renal tubular and of intestinal phosphate transport.

B-RAF contributes to the pathophysiology of polycystic kidney disease (PKD), a disorder with formation of renal cysts (Wallace 2011). The cysts are enlarged by cAMP, which is effective by stimulating epithelial cell proliferation and transepithelial fluid secretion (Wallace 2011). The influence of cAMP on cell proliferation is apparently secondary to stimulation of B-RAF, as AKT-dependent inhibition of B-RAF is disrupted in PKD (Wallace 2011). Whether or not, B-RAF is exclusively involved in the regulation of cell proliferation or, in addition, participates

in the regulation of renal tubular transport of substrates, electrolytes, and fluid, remains to be established.

In conclusion, B-RAF increases the cell surface protein abundance and activity of the type II  $\text{Na}^+$ -coupled phosphate transporters NaPi-IIa and NaPi-IIb. The stimulation of NaPi-IIa may become relevant in polycystic kidney disease, a disorder with increased B-RAF activity.

**Acknowledgments** The authors acknowledge the meticulous preparation of the manuscript by Lejla Subasic and Tanja Loch, and technical support by Elfriede Faber. This study was supported by the Deutsche Forschungsgemeinschaft, GRK 1302, SFB 773 B4/A1, La 315/13-3.

## References

Alesutan IS, Ureche ON, Laufer J, Klaus F, Zurn A, Lindner R, Strutz-Seebohm N, Tavare JM, Boehmer C, Palmada M, Lang UE, Seebohm G, Lang F (2010) Regulation of the glutamate transporter EAAT4 by PIKfyve. *Cell Physiol Biochem* 25:187–194

Alesutan I, Sopjani M, Munoz C, Fraser S, Kemp BE, Foller M, Lang F (2011) Inhibition of connexin 26 by the AMP-activated protein kinase. *J Membr Biol* 240:151–158

Alesutan I, Sopjani M, Dermaku-Sopjani M, Munoz C, Voelkl J, Lang F (2012) Upregulation of Na-coupled glucose transporter SGLT1 by Tau tubulin kinase 2. *Cell Physiol Biochem* 30:458–465

Allon M (1992) Effects of insulin and glucose on renal phosphate reabsorption: interactions with dietary phosphate. *J Am Soc Nephrol* 2:1593–1600

Almilaji A, Munoz C, Hosseinzadeh Z, Lang F (2013a) Upregulation of Na, Cl-coupled betaine/gamma-amino-butyric acid transporter BGT1 by Tau tubulin kinase 2. *Cell Physiol Biochem* 32:334–343

Almilaji A, Szteyn K, Fein E, Pakladok T, Munoz C, Elvira B, Towhid ST, Alesutan I, Shumilina E, Bock CT, Kandolf R, Lang F (2013b) Down-regulation of  $\text{Na}/\text{K}^+$  ATPase activity by human parvovirus B19 capsid protein VP1. *Cell Physiol Biochem* 31:638–648

Bacic D, Schulz N, Biber J, Kaissling B, Murer H, Wagner CA (2003) Involvement of the MAPK-kinase pathway in the PTH-mediated regulation of the proximal tubule type IIa  $\text{Na}/\text{Pi}$  cotransporter in mouse kidney. *Pflugers Arch* 446:52–60

Bacic D, Lehir M, Biber J, Kaissling B, Murer H, Wagner CA (2006) The renal  $\text{Na}/\text{Pi}$  cotransporter NaPi-IIa is internalized via the receptor-mediated endocytic route in response to parathyroid hormone. *Kidney Int* 69:495–503

Beck L, Leroy C, Salaun C, Margall-Ducos G, Desdouets C, Friedlander G (2009) Identification of a novel function of PiT1 critical for cell proliferation and independent of its phosphate transport activity. *J Biol Chem* 284:31363–31374

Bhandaru M, Kempe DS, Rotte A, Capuano P, Pathare G, Sopjani M, Alesutan I, Tyan L, Huang DY, Siraskar B, Judenhofer MS, Stange G, Pichler BJ, Biber J, Quintanilla-Martinez L, Wagner CA, Pearce D, Foller M, Lang F (2011) Decreased bone density and increased phosphaturia in gene-targeted mice lacking functional serum- and glucocorticoid-inducible kinase 3. *Kidney Int* 80:61–67

Biber J, Hernando N, Forster I, Murer H (2009) Regulation of phosphate transport in proximal tubules. *Pflugers Arch* 458:39–52

Bogatikov E, Munoz C, Pakladok T, Alesutan I, Shojaiyefard M, Seebohm G, Foller M, Palmada M, Bohmer C, Broer S, Lang F (2012) Up-regulation of amino acid transporter SLC6A19

activity and surface protein abundance by PKB/Akt and PIKfyve. *Cell Physiol Biochem* 30:1538–1546

Broer S, Broer A, Hamprecht B (1994) Expression of Na<sup>+</sup>-independent isoleucine transport activity from rat brain in *Xenopus laevis* oocytes. *Biochim Biophys Acta* 1192:95–100

Busch AE, Wagner CA, Schuster A, Waldegger S, Biber J, Murer H, Lang F (1995) Properties of electrogenic Pi transport by a human renal brush border Na<sup>+</sup>/Pi transporter. *J Am Soc Nephrol* 6:1547–1551

Carranza A, Musolino PL, Villar M, Nowicki S (2008) Signaling cascade of insulin-induced stimulation of L-dopa uptake in renal proximal tubule cells. *Am J Physiol Cell Physiol* 295:C1602–C1609

Chen DR, Chien SY, Kuo SJ, Teng YH, Tsai HT, Kuo JH, Chung JG (2010) SLC34A2 as a novel marker for diagnosis and targeted therapy of breast cancer. *Anticancer Res* 30:4135–4140

Davies H, Bignell GR, Cox C, Stephens P, Edkins S, Clegg S, Teague J, Woffendin H, Garnett MJ, Bottomley W, Davis N, Dicks E, Ewing R, Floyd Y, Gray K, Hall S, Hawes R, Hughes J, Kosmidou V, Menzies A, Mould C, Parker A, Stevens C, Watt S, Hooper S, Wilson R, Jayatilake H, Gusterson BA, Cooper C, Shipley J, Hargrave D, Pritchard-Jones K, Maitland N, Chenevix-Trench G, Riggins GJ, Bigner DD, Palmieri G, Cossu A, Flanagan A, Nicholson A, Ho JW, Leung SY, Yuen ST, Weber BL, Seigler HF, Darrow TL, Paterson H, Marais R, Marshall CJ, Wooster R, Stratton MR, Futreal PA (2002) Mutations of the BRAF gene in human cancer. *Nature* 417:949–954

De Luca A, Maiello MR, D'Alessio A, Pergameno M, Normanno N (2012) The RAS/RAF/MEK/ERK and the PI3 K/AKT signalling pathways: role in cancer pathogenesis and implications for therapeutic approaches. *Expert Opin Ther Targets* 16(Suppl 2):S17–S27

DeFronzo RA, Goldberg M, Agus ZS (1976) The effects of glucose and insulin on renal electrolyte transport. *J Clin Invest* 58:83–90

Dermaku-Sopjani M, Sopjani M, Saxena A, Shojaiefard M, Bogatikov E, Alesutan I, Eichenmuller M, Lang F (2011) Downregulation of NaPi-IIa and NaPi-IIb Na-coupled phosphate transporters by coexpression of Klotho. *Cell Physiol Biochem* 28:251–258

Dieter M, Palmada M, Rajamanickam J, Aydin A, Busjahn A, Boehmer C, Luft FC, Lang F (2004) Regulation of glucose transporter SGLT1 by ubiquitin ligase Nedd4-2 and kinases SGK1, SGK3, and PKB. *Obes Res* 12:862–870

Eisenhardt AE, Olbrich H, Roring M, Janzarik W, Anh TN, Cin H, Remke M, Witt H, Korshunov A, Pfister SM, Omran H, Brummer T (2011) Functional characterization of a BRAF insertion mutant associated with pilocytic astrocytoma. *Int J Cancer* 129:2297–2303

Feld S, Hirschberg R (1996) Insulin like growth factor I and the kidney. *Trends Endocrinol Metab* 7:85–93

Ferreira Francisco FA, Pereira e Silva JL, Hochegger B, Zanetti G, Marchiori E (2013) Pulmonary alveolar microlithiasis. State-of-the-art review. *Respir Med* 107:1–9

Foller M, Kempe DS, Boini KM, Pathare G, Siraskar B, Capuano P, Alesutan I, Sopjani M, Stange G, Mohebbi N, Bhandaru M, Ackermann TF, Judenhofer MS, Pichler BJ, Biber J, Wagner CA, Lang F (2011) PKB/SGK-resistant GSK3 enhances phosphaturia and calcaturia. *J Am Soc Nephrol* 22:873–880

Green CJ, Goransson O, Kular GS, Leslie NR, Gray A, Alessi DR, Sakamoto K, Hundal HS (2008) Use of Akt inhibitor and a drug-resistant mutant validates a critical role for protein kinase B/Akt in the insulin-dependent regulation of glucose and system A amino acid uptake. *J Biol Chem* 283:27653–27667

Henrion U, Zumhagen S, Steinke K, Strutz-Seebohm N, Stallmeyer B, Lang F, Schulze-Bahr E, Seebohm G (2012) Overlapping cardiac phenotype associated with a familial mutation in the voltage sensor of the KCNQ1 channel. *Cell Physiol Biochem* 29:809–818

Hilfiker H, Hattenhauer O, Traebert M, Forster I, Murer H, Biber J (1998) Characterization of a murine type II sodium–phosphate cotransporter expressed in mammalian small intestine. *Proc Natl Acad Sci USA* 95:14564–14569

Hosseinzadeh Z, Bhavsar SK, Lang F (2012a) Down-regulation of the myoinositol transporter SMIT by JAK2. *Cell Physiol Biochem* 30:1473–1480

Hosseinzadeh Z, Bhavsar SK, Lang F (2012b) Downregulation of CIC-2 by JAK2. *Cell Physiol Biochem* 29:737–742

Hosseinzadeh Z, Dong L, Bhavsar SK, Warsi J, Almilaji A, Lang F (2013a) Upregulation of peptide transporters PEPT1 and PEPT2 by Janus kinase JAK2. *Cell Physiol Biochem* 31:673–682

Hosseinzadeh Z, Sopjani M, Pakladok T, Bhavsar SK, Lang F (2013b) Downregulation of KCNQ4 by Janus kinase 2. *J Membr Biol* 246:335–341

Hu MC, Shi M, Zhang J, Pastor J, Nakatani T, Lanske B, Razzaque MS, Rosenblatt KP, Baum MG, Kuro-o M, Moe OW (2010) Klotho: a novel phosphaturic substance acting as an autocrine enzyme in the renal proximal tubule. *FASEB J* 24:3438–3450

Ishiki M, Klip A (2005) Minireview: recent developments in the regulation of glucose transporter-4 traffic: new signals, locations, and partners. *Endocrinology* 146:5071–5078

Jarzab B, Wiench M, Fujarewicz K, Simek K, Jarzab M, Oczko-Wojciechowska M, Włoch J, Czarniecka A, Chmielik E, Lange D, Pawlaczek A, Szpak S, Gubala E, Swierniak A (2005) Gene expression profile of papillary thyroid cancer: sources of variability and diagnostic implications. *Cancer Res* 65:1587–1597

Jehle AW, Forgo J, Biber J, Lederer E, Krapf R, Murer H (1998) IGF-I and vanadate stimulate Na/Pi-cotransport in OK cells by increasing type II Na/Pi-cotransporter protein stability. *Pflugers Arch* 437:149–154

Kamata T, Pritchard C (2011) Mechanisms of aneuploidy induction by RAS and RAF oncogenes. *Am J Cancer Res* 1:955–971

Kempe DS, Ackermann TF, Boini KM, Klaus F, Umbach AT, Dermaku-Sopjani M, Judenhofer MS, Pichler BJ, Capuano P, Stange G, Wagner CA, Birnbaum MJ, Pearce D, Foller M, Lang F (2010a) Akt2/PKBbeta-sensitive regulation of renal phosphate transport. *Acta Physiol (Oxf)* 200:75–85

Kempe DS, Dermaku-Sopjani M, Frohlich H, Sopjani M, Umbach A, Puchchakayala G, Capasso A, Weiss F, Stubs M, Foller M, Lang F (2010b) Rapamycin-induced phosphaturia. *Nephrol Dial Transplant* 25:2938–2944

Lee IH, Dinudom A, Sanchez-Perez A, Kumar S, Cook DI (2007) Akt mediates the effect of insulin on epithelial sodium channels by inhibiting Nedd4-2. *J Biol Chem* 282:29866–29873

Lim SK, Park MJ, Jung HK, Park AY, Kim DI, Kim JC, Bae CS, Kim KY, Yoon KC, Han HJ, Park SH (2008) Bradykinin stimulates glutamate uptake via both B1R and B2R activation in a human retinal pigment epithelial cells. *Life Sci* 83:761–770

Mannack G, Graf D, Donner MM, Richter L, Gorg B, Vom Dahl S, Haussinger D, Schliess F (2008) Taurolithocholic acid-3 sulfate impairs insulin signaling in cultured rat hepatocytes and perfused rat liver. *Cell Physiol Biochem* 21:137–150

Marks J, Debnam ES, Unwin RJ (2010) Phosphate homeostasis and the renal-gastrointestinal axis. *Am J Physiol Renal Physiol* 299:F285–F296

Mia S, Munoz C, Pakladok T, Siraskar G, Voelkl J, Alesutan I, Lang F (2012) Downregulation of Kv1.5 K channels by the AMP-activated protein kinase. *Cell Physiol Biochem* 30:1039–1050

Munoz C, Almilaji A, Setiawan I, Foller M, Lang F (2013) Upregulation of the inwardly rectifying K<sup>+</sup> channel Kir2.1 (KCNJ2) by protein kinase B (PKB/Akt) and PIKfyve. *J Membr Biol* 246:189–197

Murer H, Hernando N, Forster I, Biber J (2000) Proximal tubular phosphate reabsorption: molecular mechanisms. *Physiol Rev* 80:1373–1409

Murer H, Forster I, Biber J (2004) The sodium phosphate cotransporter family SLC34. *Pflugers Arch* 447:763–767

Murillo-Cuesta S, Rodriguez-de la Rosa L, Cediol R, Lassaletta L, Varela-Nieto I (2011) The role of insulin-like growth factor-I in the physiopathology of hearing. *Front Mol Neurosci* 4:11

Nielsen LB, Pedersen FS, Pedersen L (2001) Expression of type III sodium-dependent phosphate transporters/retroviral receptors mRNAs during osteoblast differentiation. *Bone* 28:160–166

Nowik M, Picard N, Stange G, Capuano P, Tenenhouse HS, Biber J, Murer H, Wagner CA (2008) Renal phosphaturia during metabolic acidosis revisited: molecular mechanisms for decreased renal phosphate reabsorption. *Pflugers Arch* 457:539–549

Pakladok T, Hosseinzadeh Z, Alesutan I, Lang F (2012) Stimulation of the Na(+)–coupled glucose transporter SGLT1 by B-RAF. *Biochem Biophys Res Commun* 427:689–693

Pakladok T, Almilaji A, Munoz C, Alesutan I, Lang F (2013) PIKfyve sensitivity of hERG channels. *Cell Physiol Biochem* 31:785–794

Parkin DM, Bray F (2006) Chapter 2: the burden of HPV-related cancers. *Vaccine* 24(Suppl 3:S3):11–25

Rangel LB, Sherman-Baust CA, Wernyj RP, Schwartz DR, Cho KR, Morin PJ (2003) Characterization of novel human ovarian cancer-specific transcripts (HOSTs) identified by serial analysis of gene expression. *Oncogene* 22:7225–7232

Roring M, Brummer T (2012) Aberrant B-Raf signaling in human cancer—10 years from bench to bedside. *Crit Rev Oncog* 17:97–121

Shojaiefard M, Hosseinzadeh Z, Bhavsar SK, Lang F (2012) Downregulation of the creatine transporter SLC6A8 by JAK2. *J Membr Biol* 245:157–163

Strutz-Seebohm N, Pusch M, Wolf S, Stoll R, Tapken D, Gerwert K, Attali B, Seebohm G (2011) Structural basis of slow activation gating in the cardiac I<sub>Ks</sub> channel complex. *Cell Physiol Biochem* 27:443–452

Tanner S, Shen Z, Ng J, Florea L, Guigo R, Briggs SP, Bafna V (2007) Improving gene annotation using peptide mass spectrometry. *Genome Res* 17:231–239

Vaughan-Jones RD, Swietach P (2008) Pushing and pulling the cardiac sodium/hydrogen exchanger. *Circ Res* 103:773–775

Villa-Bellosta R, Ravera S, Sorribas V, Stange G, Levi M, Murer H, Biber J, Forster IC (2009) The Na<sup>+</sup>–Pi cotransporter PiT-2 (SLC20A2) is expressed in the apical membrane of rat renal proximal tubules and regulated by dietary Pi. *Am J Physiol Renal Physiol* 296:F691–F699

Wallace DP (2011) Cyclic AMP-mediated cyst expansion. *Biochim Biophys Acta* 1812:1291–1300

Wan PT, Garnett MJ, Roe SM, Lee S, Niculescu-Duvaz D, Good VM, Jones CM, Marshall CJ, Springer CJ, Barford D, Marais R, Cancer Genome Project (2004) Mechanism of activation of the RAF-ERK signaling pathway by oncogenic mutations of B-RAF. *Cell* 116:855–867

Warsi J, Hosseinzadeh Z, Dong L, Pakladok T, Umbach AT, Bhavsar SK, Shumilina E, Lang F (2013) Effect of Janus kinase 3 on the peptide Transporters PEPT1 and PEPT2. *J Membr Biol* 246:885–892

Whiteman EL, Cho H, Birnbaum MJ (2002) Role of Akt/protein kinase B in metabolism. *Trends Endocrinol Metab* 13:444–451

Xu H, Inouye M, Hines ER, Collins JF, Ghishan FK (2003) Transcriptional regulation of the human NaPi-IIb cotransporter by EGF in Caco-2 cells involves c-myb. *Am J Physiol Cell Physiol* 284:C1262–C1271